cGMP-Prkg1 signaling and Pde5 inhibition shelter cochlear hair cells and hearing function

Mirko Jaumann[1], Juliane Dettling[1], Martin Gubelt[1], Ulrike Zimmermann[1], Andrea Gerling[2], François Paquet-Durand[3], Susanne Feil[2], Stephan Wolpert[1], Christoph Franz[1], Ksenya Varakina[1], Hao Xiong[1], Niels Brandt[4,5], Stephanie Kuhn[4,9], Hyun-Soon Geisler[1], Karin Rohbock[1], Peter Ruth[6], Jens Schlossmann[7], Joachim Hütter[8], Peter Sandner[8], Robert Feil[2], Jutta Engel[4,5], Marlies Knipper[1] & Lukas Rüttiger[1]

Noise-induced hearing loss (NIHL) is a global health hazard with considerable pathophysiological and social consequences that has no effective treatment. In the heart, lung and other organs, cyclic guanosine monophosphate (cGMP) facilitates protective processes in response to traumatic events. We therefore analyzed NIHL in mice with a genetic deletion of the gene encoding cGMP-dependent protein kinase type I (*Prkg1*) and found a greater vulnerability to and markedly less recovery from NIHL in these mice as compared to mice without the deletion. Prkg1 was expressed in the sensory cells and neurons of the inner ear of wild-type mice, and its expression partly overlapped with the expression profile of cGMP-hydrolyzing phosphodiesterase 5 (Pde5). Treatment of rats and wild-type mice with the Pde5 inhibitor vardenafil almost completely prevented NIHL and caused a Prkg1-dependent upregulation of poly (ADP-ribose) in hair cells and the spiral ganglion, suggesting an endogenous protective cGMP-Prkg1 signaling pathway that culminates in the activation of poly (ADP-ribose) polymerase. These data suggest vardenafil or related drugs as possible candidates for the treatment of NIHL.

Hearing impairment is a rapidly growing healthcare issue that currently affects about 190 million people in industrialized countries, a number that is expected to rise to 700 million by 2050. The reasons behind these increasing numbers are demographic changes in industrial societies and the rising number of affected people in the younger population, a phenomenon possibly connected to the negligent use of portable audio players. Excessive noise damages the sensory hair cells in the ears that are generated in mammals only during embryonic development[1] and that do not regenerate. In addition, even minor hearing loss is often connected to the slow degeneration of auditory nerve fibers, which is not always detected by conventional clinical threshold testing[2]. Because spontaneous regeneration does not take place, cell-protective therapies are needed to prevent hearing loss. For non-sensory disorders, inhibitors of cGMP-specific PDEs have emerged as powerful drugs to treat erectile dysfunction, pulmonary hypertension (for reviews, see refs. 3,4) and, recently, benign prostatic hyperplasia[5].

cGMP acts on specific receptor proteins, including cGMP-dependent protein kinases (Prkg, also referred to as cGK or PKG). Mammals have two *Prkg* genes that encode the cytosolic Prkg type I (*Prkg1*) with two isoforms expressed (Prkg1α and Prkg1β) and the membrane-associated Prkg type II (*Prkg2*). Prkg1 is expressed in neuronal and non-neuronal cell types, including guinea pig cochlea supporting cells and spiral ganglion neurons (SGNs)[6], whereas Prkg2 is expressed in intestinal mucosa, kidney juxtaglomerular cells and chondrocytes[7,8]. Hydrolysis of the second messenger molecule cGMP by PDEs terminates the signal. Consequently, cGMP-mediated pathways can be stimulated by Pde5 inhibitors such as sildenafil or vardenafil.

Here we show that Prkg1 and Pde5 are expressed together in cochlear hair cells. Using a combined genetic and pharmacological approach, we identify a protective cGMP-Prkg1 signaling cascade in the inner ear and suggest the use of Pde5 inhibitors as a potentially new therapeutic approach to protect sensory and neuronal tissue from NIHL.

RESULTS

Pde5 and Prkg1 expression in the cochlea

We studied mRNA and protein expression of Prkg1 and Pde5 in cochlear hair cells and neurons. We used RT-PCR with either *Pde5*- or *Prkg1*-specific primers on complementary DNA (cDNA) obtained from cochlear tissue or nested RT-PCR with cDNA from isolated outer hair cells (OHC) and inner hair cells (IHC). The expected PCR products (**Fig. 1a**) of *Pde5* and *Prkg1* were amplified

Figure 1 Prkg1 and Pde5 expression in the cochlea. (**a**) RT-PCR with cDNA from cochlear tissue. The expected products were amplified with primers for *Pde5* (354 bp), *Prkg1* (248 bp), *Prkg1a* (446 bp) and *Prkg1b* (361 bp). Nested RT-PCR amplified products can be seen for *Pde5* (215 bp) in basal but not apical OHCs, for *Prkg1* (160 bp) in apical OHCs, for *Prkg1a* (245 bp) in basal but not apical OHCs and for *Prkg1b* in basal (130 bp) and apical OHCs (361 bp). Glyceraldehyde 3-phosphate dehydrogenase (GAPDH) or cyclophilin (CP) were used as loading controls. Nested RT-PCR amplified products with primers for *Pde5* (215 bp) and *Prkg1* (160 bp) in IHCs. (**b**) Western blot for Pde5 in cochleae of 3-week-old rats (Co) and expression of Prkg1α and Prkg1β proteins in the mouse cochlea (mCo) using a general antibody to Prkg1 and isoform-specific antibodies to Prkg1α and Prkg1β. Immunoblotting of recombinant Prkg1α and Prkg1β proteins (rec. α and rec. β) and of cochlear tissue from Prkg1-deficient mice (KO), with actin used as the loading control. (**c,d**) Pde5 labeling (red) of cochlear whole-mount preparations (**c**, co-labeled for the OHC-marker prestin, shown in green, from a top view) in the supranuclear region below the stereocilia (**d**, co-labeled for the stereocilia marker Eps8, shown with an arrow and in green, from a side view). (**e**) Pde5 localization at the synaptic region of IHCs (co-labeled for the neuronal marker NF200, shown in green). (**f**) Pde5 expression in somata of SGNs (co-labeled for the neuronal marker NF200, shown in green). Images in **c**–**f** represent maximum intensity projections over all layers of three-dimensionally deconvoluted image stacks. Mouse tissue is shown in **c** and **d**, and rat tissue is shown in **e** and **f**. Scale bars, **c,d**, 5 μm; **e,f**, 10 μm.
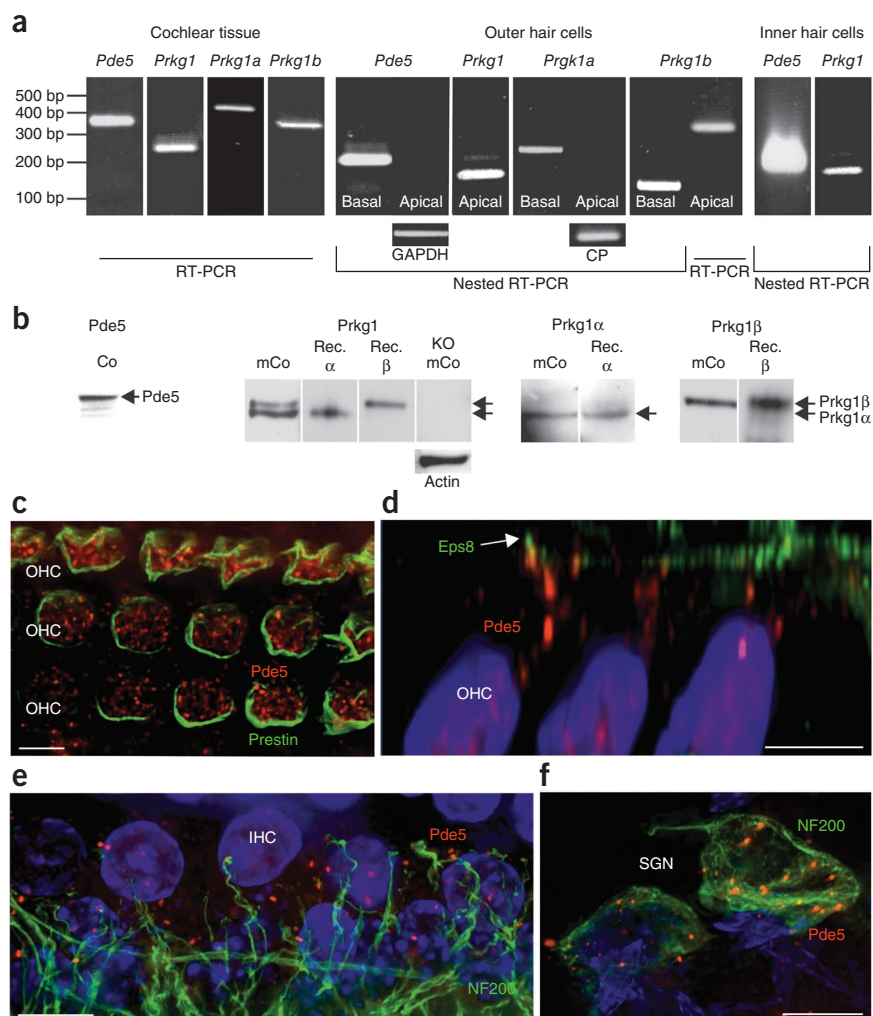
in cochlear tissue, and we detected both of the *Prkg1* isoforms in the PCR product (*Prkg1a* and *Prkg1b*). We analyzed two types of isolated cochlear OHCs: apical (low-frequency processing turn) OHCs and midbasal and basal (high-frequency processing turn) OHCs. Using nested RT-PCR, the expected products (**Fig. 1a**) of *Pde5*, *Prkg1a* and *Prkg1b* were amplified in midbasal and basal OHCs. Using nested RT-PCR, the expected products of *Prkg1* were amplified in apical OHCs. Using RT-PCR, the *Prkg1b* isoform was amplified in apical OHCs. Using nested RT-PCR on cDNA from isolated IHCs, the expected products of both *Pde5* and *Prkg1* were amplified (**Fig. 1a**).

A western blot analysis on cochlear tissue from mature rats identified Pde5 as an immunoreactive band with a molecular weight of ~96 kDa (**Fig. 1b**)[9]. We studied Prkg1 protein expression in cochlear tissue from 5-week-old control and Prkg1-deficient mice (**Fig. 1b**). We used a general antibody to Prkg1, which detects both the Prkg1α (76 kD) and Prkg1β (78 kD) isoforms[10], and isoform-specific antibodies to Prkg1α and Prkg1β. The general antibody to Prkg1 detected both of the Prkg1 isoforms in rat and mouse cochlear tissue and also detected recombinant Prkg1α and Prkg1β proteins but showed no signal in tissue from Prkg1-deficient mice (**Fig. 1b**). We showed the specificity of the isoform-specific antibodies using recombinant Prkg1α and recombinant Prkg1β proteins as positive controls, and we detected both isoforms in mouse cochlear tissue (**Fig. 1b**).

Pde5 and Prkg1 protein localization

We stained Pde5 and Prkg1 protein in cochlear hair cells, SGNs and satellite cells (**Figs. 1** and **2**). We showed localization using immunofluorescent staining of whole-mount preparations and cryosections co-labeled with antibodies against hair-cell–specific markers (the OHC marker prestin and the stereocilia markers epidermal growth factor receptor pathway substrate 8 (Eps8) (ref. 11) and whirlin[12]; **Fig. 1c,d** and **Fig. 2a,b**), a neuronal marker (NF200; **Fig. 1e,f**) and a supporting cell marker (K_{ir}4.1, which labeled the myelin sheaths of satellite cells wrapping the somata of the SGNs[13]; **Fig. 2f,g**). Pde5 protein was cytoplasmatically localized in the supranuclear region below the cuticular plate in the OHCs (**Fig. 1c,d** and **Fig. 2a**), in a dot-like pattern at the level of the IHC synapse (**Fig. 1e**) and in SGNs (**Fig. 1f**). With the general antibody to Prkg1, we found a similar subcellular localization in OHCs (**Fig. 2b**) and IHCs (data not shown). The isoform-specific antibody to Prkg1β stained the SGNs (**Fig. 2c–g**) and satellite cells (**Fig. 2g**). We did not observe Prkg1 immunopositive signals in Prkg1-deficient mice (**Fig. 2b,e**).

In summary, Pde5 and Prkg1 are expressed in IHCs, OHCs and SGNs, and Prkg1 (and perhaps Pde5) is also expressed in the SGNs surrounding the satellite cells of the mature inner ear.

Prkg1-deficient mice have less recovery from noise damage

Prkg1-deficient mice have normal hearing thresholds (**Supplementary Fig. 1a**). However, noise exposure led to significantly more hearing
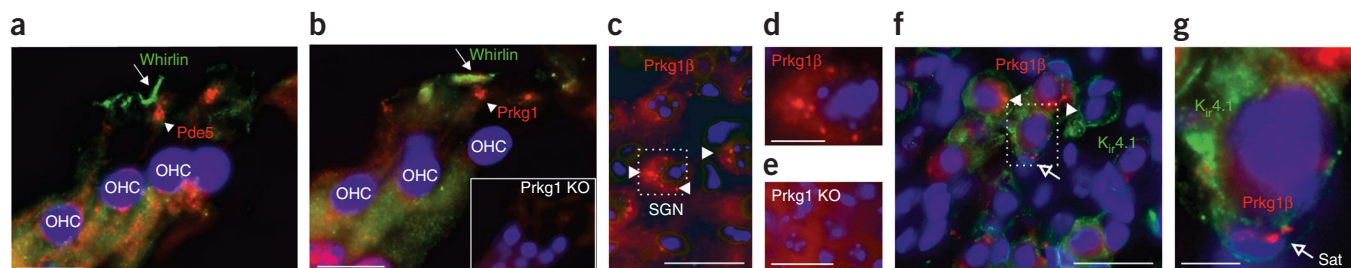
Figure 2 Pde5 and Prkg1 localization in the cochlea. (**a**) Pde5 localization at the supranuclear level in OHCs in cochlear cryosections (red and arrowhead) (the stereocilia were stained for whirlin, indicated with an arrow and shown in green). (**b**) Localization of Prkg1 protein (red and arrowhead) (co-labeled for whirlin, indicated with an arrow and shown in green). No signals of antibodies specific to Prkg1 were seen in Pkg1-deficient mice (inset). (**c**) Specific dot-like staining in SGNs with antibodies specific to Prkg1β in spiral ganglion (red and arrowheads), shown in higher magnification in **d**. (**e**) No Prkg1 antibody signals were in Prkg1-deficient mice. (**f**) Co-labeling of Prkg1β (red) with the supporting cell marker $K_{ir}4.1$ (green) showing Prkg1β expression in $K_{ir}4.1$-positive satellite cells (closed arrowhead), as shown in higher magnification in **g** (open arrow). Mouse tissue is shown in **a**–**g**. Scale bars, **a**,**b**, 10 μm; **c**,**f**, 20 μm; **d**,**e**,**g**, 5 μm. (**h**) Vulnerability of 7-week-old Prkg1-deficient mice ($n = 8$) and littermate controls ($n = 7$) to noise, as shown by recovery of ABR thresholds after noise exposure. TTS, temporary threshold shift. $P = 0.0226$ by multivariate analysis of variance (MANOVA). *$P < 0.05$, **$P < 0.01$ by t test with Bonferroni-Holms correction. (**i**) Function of OHCs in Prkg1-deficient and control mice after acoustic trauma. DPOAE amplitudes in Prkg1-deficient (before trauma, $n = 9$; after trauma, $n = 6$) and control mice (before trauma, $n = 7$; after trauma, $n = 7$). $P = 0.001$ by one-way ANOVA. *$P < 0.05$, **$P < 0.01$, NS, not significant by Bonferroni's multiple comparison test. Data are mean ± s.e.m.
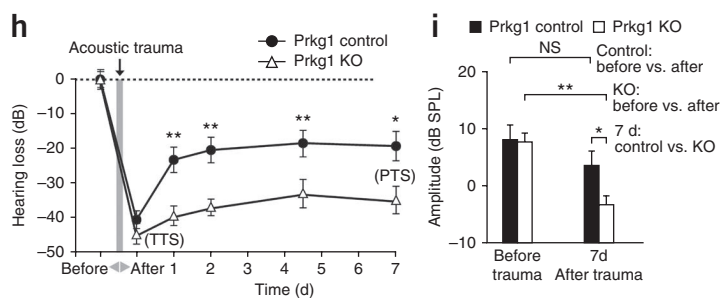
loss in these mice than in control mice not deficient in Prkg1 (**Fig. 2h**). Immediately after noise exposure, the temporary hearing threshold shift was 41 dB and 46 dB for the control and Prkg1-deficient mice, respectively ($P = 0.16$). At 1 d after the noise exposure, the mice's hearing thresholds had for the most part recovered from the temporary shift and the hearing loss in Prkg1-deficient mice was significantly greater than in control mice. At 7 d after trauma, the amount of permanent hearing loss (permanent threshold shift) was significantly higher in Prkg1-deficient mice (35 dB) than in control mice (19 dB; $P = 0.0152$) (**Fig. 2h** and **Supplementary Fig. 1b**). Prkg1-deficient mice are therefore more vulnerable to noise and may have less capacity to recover from temporary noise trauma than control mice.

Noise exposure damages the OHCs. The greater amount of damage to the OHCs in Prkg1-deficient mice became apparent after

observing significantly greater reductions in distortion products of otoacoustic emissions (DPOAEs) in these mice than in control mice 7 d after noise exposure (**Fig. 2i** and **Supplementary Fig. 1c**). We investigated the integrity of the OHCs before (**Fig. 3**) and 1 week after noise exposure using epifluorescence microscopy in cryosectioned cochleae of Prkg1-deficient and control mice stained for Kcnq4 (**Fig. 3**) and voltage- and Ca^{2+}-activated K$^+$ (BKCa) (**Fig. 4a–d**) channels. Kcnq4 channels mediate the dominant K$^+$ current in OHCs ($I_{K,n}$) and are therefore responsible for setting their resting potential and for repolarizing the OHC receptor potential[14,15]. The BKCa channels are localized in the basal part of the OHCs, just opposite of the efferent presynapses[16]. Both BKCa and Kcnq4 ion channels are required for normal hearing and have been suggested to protect OHCs in cochlear regions
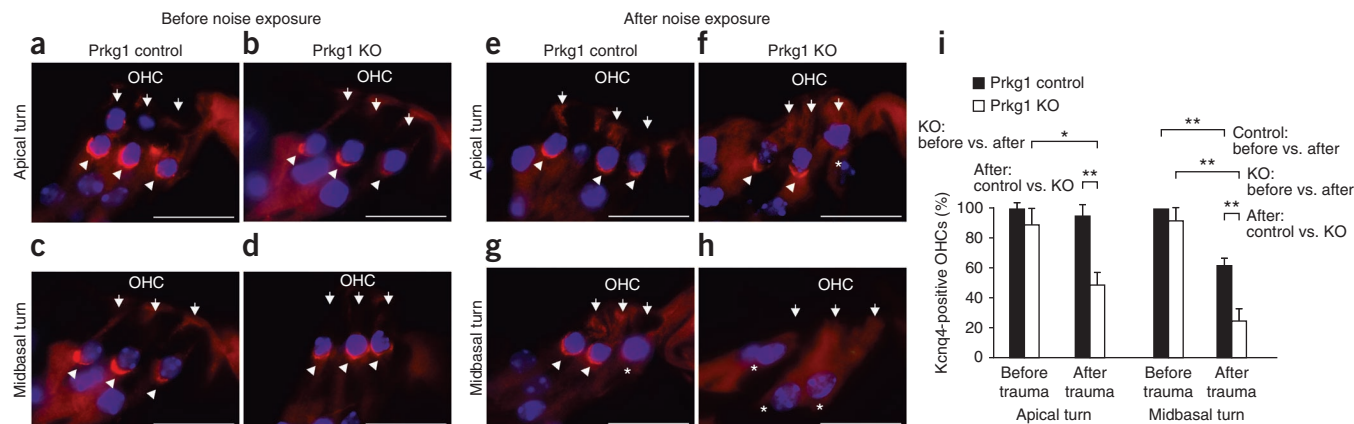
Figure 3 Immunohistochemical staining for Kcnq4 protein in control and Prkg1-deficient mice. (**a**–**d**) Kcnq4 labeling (arrowheads) in cochlear outer hair cells (arrows) before noise exposure. (**e**–**i**) The effect of noise exposure on the number of OHCs and Kcnq4-positive cells (Kcnq4-positive cells are indicated with arrows, and Kcnq4-negative cells are indicated with stars), and the quantification of Kcnq4 positive cells (**i**), in Prkg1-deficient (before exposure, $n = 4$; after exposure, $n = 6$) and control mice (before exposure, $n = 4$; after exposure, $n = 6$). Data are mean ± s.e.m. *$P < 0.05$, **$P < 0.01$ by Mann-Whitney U test. Scale bars, 20 μm.

Figure 4 Vardenafil treatment during NIHL. (**a**–**d**) Immunohistochemical staining for BKCa protein (arrowheads) in OHC (arrows) of control and Prkg1-deficient mice. Effect of noise exposure (4–16 kHz, wi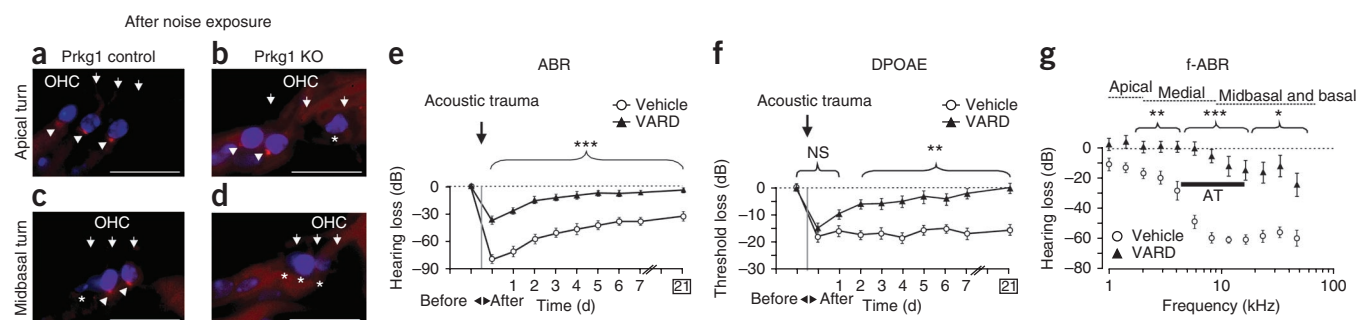th a two-octave band-noise stimulus of 120 dB SPL for 1 h) on the number of OHCs and the reduction of BKCa-positive cells in Prkg1-deficient (**b**,**d**) and control mice (**a**,**c**) (7 d after noise exposure, the stars indicate that no BKCa signal was detected). (**e**,**f**) ABR threshold (**e**) and DPOAEs (**f**) in vehicle-treated (circles) and vardenafil-pretreated (VARD, triangles) 3- to 5-month-old rats as a function of time before, immediately after and at days 1–21 after noise exposure (acoustic trauma). $P < 0.0001$ by MANOVA for both ABR thresholds and DPOAEs. (**g**) Frequency-specific ABR (f-ABR) thresholds 21 days after noise exposure. Data are mean ± s.e.m. (vehicle-treated rats, $n = 9$–11; vardenafil-pretreated rats, $n = 10$–12). The black horizontal bar in **g** shows the frequency range of the noise stimulus. $*P < 0.05$, $**P < 0.01$, $***P < 0.001$ by t test with Bonferroni-Holms correction. NS, not significant. Scale bars, 20 μm.

that register high frequency from Ca^{2+} overload[15,17]. The surface expression of Kcnq4 and BKCa in the midbasal OHCs seems to be less after noise exposure already in control mice. The number of affected midbasal OHCs with loss of surface expression of Kcnq4 was significantly higher in Prkg1-deficient mice than in control mice (**Fig. 3i**). The loss of Kcnq4 surface expression in Prkg1-deficient mice was less pronounced in their apical cochlear turns. These findings indicate that functional and cellular damage is more pronounced in the absence of Prkg1.

Vardenafil protects from NIHL

Because cGMP-Prkg1 signaling seemed to reduce NIHL, these protective effects should be intensified by inhibition of cGMP hydrolysis. We treated rats with the highly specific Pde5 inhibitor vardenafil before

and after acoustic trauma. We saw significantly lower auditory-evoked brainstem response (ABR) thresholds in the rats pretreated with vardenafil (10 mg per kg of body weight, administered 2 h before acoustic trauma) compared to the vehicle-treated rats at 20 min after noise exposure (**Fig. 4e** and **Supplementary Fig. 2a**) and at 21 days after noise exposure (**Fig. 4e**). The DPOAEs of the rats pretreated with vardenafil recovered until day 21 after noise exposure (when we stopped measurements), whereas the DPOAEs of vehicle-treated rats did not recover (**Fig. 4f** and **Supplementary Fig. 2b,c**). After the recovery period, the frequency-specific ABR thresholds (**Fig. 4g**) were significantly better in rats pretreated with vardenafil compared to vehicle-treated rats in the range of frequencies of the acoustic trauma (4–16 kHz), as well as in the low-frequency (2–4 kHz) and high-frequency ranges (22.6–45 kHz).

Figure 5 IHC and OHC preservation after noise trauma and treatment with vardenafil. (**a**–**c**) Kcnq4 immunohistochemistry in the OHCs (three rows labeled as 1–3) of midbasal cochlear turns in cochlear whole-mount preparations of 3- to 4-month-old rats 21 d after noise exposure (AT) or sham exposure (Sham) and pretreated either with vehicle (AT + vehicle) or vardenafil (AT + VARD). Kcnq4-positive cells are labeled red. Nerve fibers are stained with NF200 antibodies (green). (**d**–**f**) Whole-mount immunohistochemistry of midbasal cochlear turns, where hair cell stereocilia bundles are visualized by phalloidin labeling of F-actin. (**g**) Average number of Ctbp2 (Ribeye)-positive dots (ribbons) ± s.e.m. in apical and medial (black bars) and midbasal and basal (white bars) cochlear turns of rats (sham exposed, $n = 6$; noise exposed plus vehicle treatment, $n = 7$; noise exposed plus vardenafil pretreatment, $n = 6$). Apical and medial, $P = 0.1608$; midbasal and basal, $P = 0.0002$ by one-way ANOVA. $**P < 0.01$, $***P < 0.001$ by Bonferroni's multiple comparison test. (**h**–**j**) Immunostaining of cochlear cryosections of 3- to 4-month-old rats (shown for the midbasal cochlear turn) with the ribbon synapse protein Ctbp2 (Ribeye) (open arrowheads, green) in sham-exposed rats (**h**), noise-exposed

vehicle-treated rats (**i**) and noise-exposed vardenafil-pretreated rats (**j**). Images in **h**–**j** represent the maximum intensity projection over all layers of the Z-stack. The cell nuclei are stained with DAPI (blue). The IHC nuclei are circled with white dotted lines. Scale bars, **a**–**c**, 50 μm; **d**–**f**, 20 μm; **h**–**j**, 10 μm.
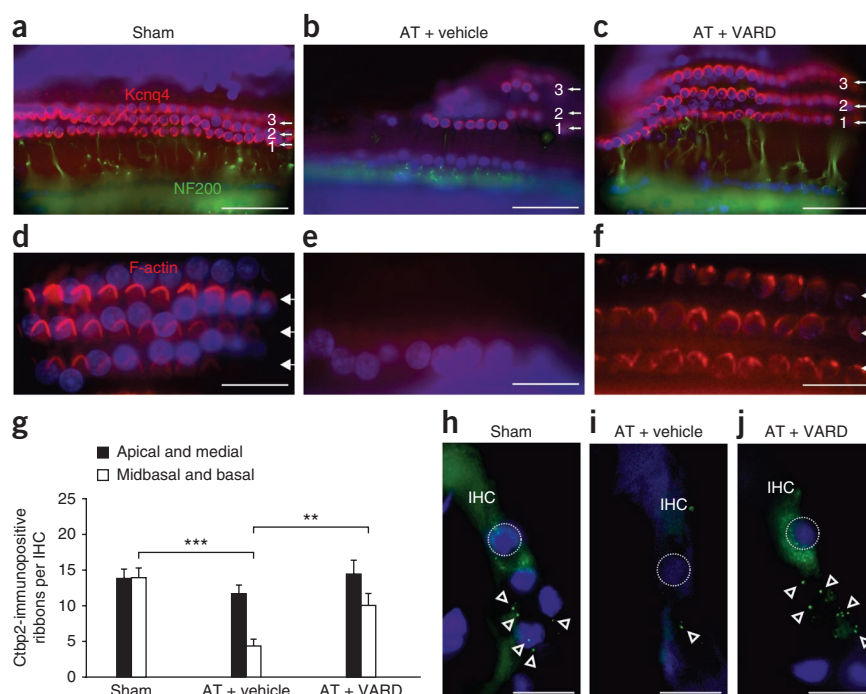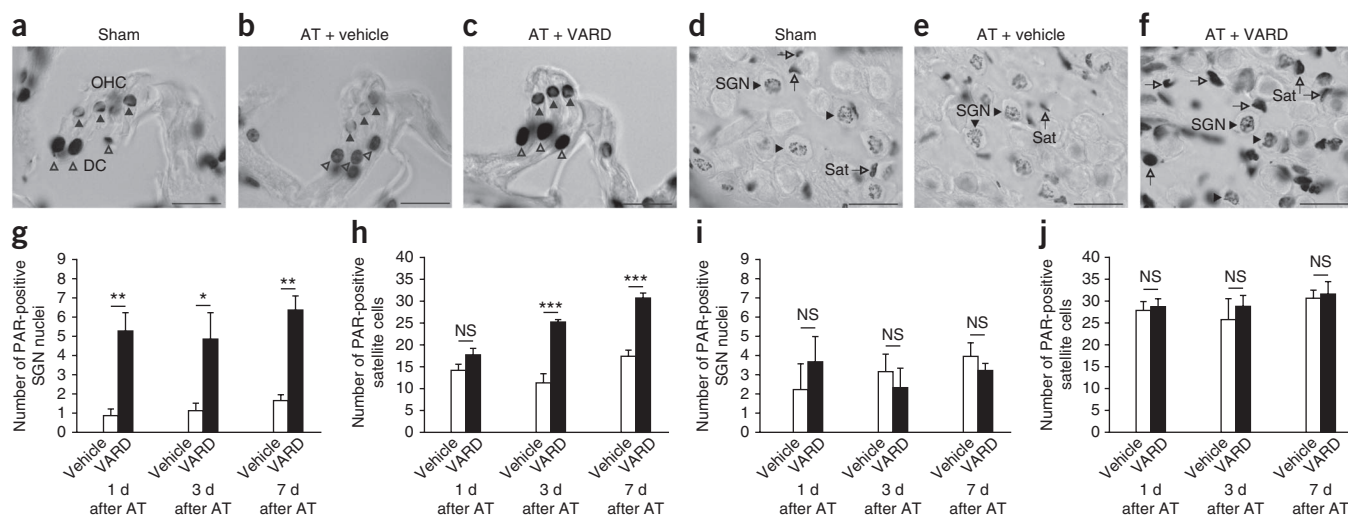
Figure 6 Parp activity after vardenafil treatment. PAR staining was performed on 3–4 month-old rats 21 d after noise exposure or sham exposure that were pretreated 2 h before exposure with either vehicle or vardenafil. (**a**–**f**) PAR staining in vardenafil-pretreated rats (**c**,**f**) in comparison to sham-exposed (**a**,**d**) and vehicle-treated rats (**b**,**e**) in outer hair cells (**a**–**c**, closed arrowheads), SGNs (**d**–**f**, closed arrowheads) and satellite cells (Sat) (**d**–**f**, open arrows). Deiters cells (DC) (**a**–**c**, open arrowheads) are indicated for orientation. (**g**–**j**) Quantitative evaluations of midbasal and basal (**g**,**h**) and apical (**i**,**j**) PAR-positive SGNs (**g**,**i**) and satellite cells (**h**,**j**) in noise-exposed rats pretreated with either vehicle or vardenafil at 1–7 d after noise exposure. $P = 0.003$ (**g**), $P < 0.0001$ (**h**), $P = 0.7809$ (**i**), and $P = 0.6613$ (**j**) by one-way ANOVA. Data are mean ± s.e.m. *$P < 0.05$, **$P < 0.01$, ***$P < 0.001$, NS, not significant after Bonferroni's multiple comparison test. Scale bars, 20 μm.

We also observed a protective effect of vardenafil on hearing function when we started vardenafil treatment in rats 6 h after noise exposure (**Supplementary Fig. 3**), with different intensities of acoustic overexposure inducing only transient hearing loss (**Supplementary Fig. 4**), as assessed by measuring the rats' ABR thresholds 7 d after exposure; we saw the same effect when we repeated the experiment in mice (**Supplementary Fig. 5**).

Vardenafil preserves hair-cell phenotype after acoustic trauma

If Pde5 inhibition protects from hearing loss through the activation of an otoprotective cGMP-Prkg1 signaling pathway in hair cells, noise-induced changes in hair-cell phenotype should be reduced in vardenafil-pretreated specimens. As described above, Kcnq4 surface expression in the OHCs is highly sensitive to noise exposure[14,15] and thus serves as a suitable marker for OHC damage (**Figs. 3g–j** and **5a–c** and **Supplementary Figs. 4b–i** and **5c–j**). We also tested the vulnerability of hair cell stereocilia to noise[18] using phalloidin labeling of F-actin (**Fig. 5d–f**). We furthermore evaluated the noise vulnerability of synaptic ribbons, specialized organelles for the facilitation of exocytosis in inner hair cells[2], by the number of C-terminal binding protein 2 (Ctbp2, also known as Ribeye)-immunopositive dots, as determined by Z-stack images (**Fig. 5g–j**).

Three weeks after noise exposure, Kcnq4 was nearly completely lost from the OHCs in the basal cochlear turn in vehicle-treated rats (**Fig. 5b**), whereas in rats pretreated with vardenafil 2 h before noise trauma, the Kcnq4 in the OHCs was preserved (**Fig. 5c**), as shown using whole-mount studies. Phalloidin labeling in whole-mount preparations at 24 h after noise exposure (**Fig. 5d–f**) was largely lost from the OHCs in the midbasal cochlear turn in vehicle-treated rats (**Fig. 5e**) but was preserved in vardenafil-pretreated rats (**Fig. 5f**).

Six to seven days after acoustic overstimulation, the IHC synapses of vehicle-treated rats showed a significant decline in the number of Ctbp2 (Ribeye)-immunopositive ribbons in their basal cochlear turns but had no significant changes in their medial and apical cochlear turns (**Fig. 5g**). When we pretreated rats with vardenafil, the number

of ribbons in their IHCs was similar to the number that we found in sham-exposed rats (**Fig. 5g–j**). In conclusion, vardenafil treatment almost completely rescued hearing function after noise exposure and prevented the loss of DPOAEs and the loss of IHC and OHC phenotypes in rats.

The otoprotective effect of vardenafil is mediated by Prkg1

To link the beneficial effects of vardenafil with potential downstream effectors of the Prkg1 pathway, we studied the presence of poly (ADP-ribose) (PAR) polymers, which are products of poly (ADP-ribose) polymerase (Parp) activity. The enzymatic activity of Parp has been shown to be involved in DNA repair and transcriptional activity in a cGMP- and Prkg1-dependent manner[19,20]. We analyzed the cochleae of noise-exposed rats that had been pretreated with either vardenafil or vehicle for PAR production (**Fig. 6**). We noted a ubiquitous basal level of PAR in the nuclei of OHCs, supporting Deiters cells (**Fig. 6a**), satellite cells and SGNs (**Fig. 6d**). We found no clear PAR-level differences in these cell types between the vehicle-treated rats exposed to either sham or noise in their midbasal cochlear turns 7 d after noise exposure (**Fig. 6b,e**). However, treatment with vardenafil led to a substantial elevation of PAR staining in the OHCs (**Fig. 6c**) as well as in the nuclei of SGNs and satellite cells after trauma (**Fig. 6f**). A quantitative analysis revealed an increasing number of PAR-positive SGN nuclei and satellite-cell nuclei over 7 days in the midbasal and basal but not the apical cochlear turns (**Fig. 6g–j**) in vardenafil-pretreated rats. We observed these same staining patterns when we repeated these experiments in mice (**Supplementary Fig. 6**). In noise-exposed Prkg1-deficient mice, we noted less PAR concentration in the OHCs and SGNs. In Prkg1-deficient mice pretreated with vardenafil, the number of PAR-positive cells did not increase after noise exposure, suggesting that Parp activation occurred downstream of cGMP-Prkg1 signaling (**Supplementary Fig. 6**).

The combined morphological and functional evidence indicates that treatment with vardenafil activated a cGMP-Prkg1 pathway that protects cochlear hair cells, supporting cells and

cells of the spiral ganglion (SGNs and satellite cells) from damage, supports their repair after noise-induced trauma or both.

DISCUSSION

PDEs shape and terminate cyclic nucleotide signaling, making them crucial regulators of cellular metabolism, as reflected, for example, in the clinical success of PDE inhibitors[21]. Here we describe for the first time, to our knowledge, expression of Pde5 protein in the cochlea and its partial co-localization with Prkg1, suggesting the presence of Pde5-cGMP-Prkg1 signaling in these cells. Furthermore, we show the potential for cGMP-Prkg1 signaling to reduce the deleterious effects of acoustic trauma and show how Pde5 inhibition may exploit this signaling pathway to further promote protection of hearing function. The therapeutic value of these findings is notable, as Pde5 inhibitors are already widely used drugs that are FDA approved for chronic use.

In Prkg1-deficient mice, the noise-induced threshold loss was associated with loss of DPOAEs and loss of the OHC phenotype, as seen by the loss of surface expression of the K^+ channels Kcnq4 and BKCa. This finding strongly supports the notion that the otoprotective effect of Pde5 inhibition is mediated through an increase in cGMP and the subsequent activation of Prkg1 in OHCs. But how is endogenous cGMP signaling stimulated under acoustic stress? And what are the molecular events downstream of Prkg1, or rather, which substrate proteins are phosphorylated and how does this counteract noise-induced hair-cell dysfunction and death?

Many studies have shown that excessive calcium (Ca^{2+}) entry, either through L-type Ca^{2+} channels[22] or through purinergic receptors[23–28], initiates hair-cell death[29,30]. Hyposmotic stress of OHCs was found to increase the intracellular Ca^{2+} concentration and nitric oxide (NO) production[31]. Notably, acoustic overexposure was shown to elevate Ca^{2+} concentrations and trigger NO release explicitly in the supranuclear part of the OHCs, where neuronal NO synthase is expressed[28,31]. Here we detected Pde5 and Prkg1 in close proximity in the same subcellular region of the OHCs, which is a requirement for the existence of a cGMP signaling complex in OHCs. It seems likely that a noise-induced increase of intracellular Ca^{2+} concentrations triggers a cascade of events that starts with the activation of NO synthase and the production of NO, which causes activation of soluble guanylyl cyclase[3], cGMP production and the subsequent activation of Prkg1. Prkg1 in turn may limit cytosolic Ca^{2+} concentrations, for example, through modulation of L-type Ca^{2+} channels[32] or Ca^{2+} sequestration into intracellular stores[33]. Indeed, *in vitro* studies have suggested a role for NO in opposing harmful Ca^{2+} concentration elevations in hair cells that were caused by acoustic overstimulation[23,28,34]. In addition, activation of Prkg1 suppresses hormone- and depolarization-induced elevations of intracellular Ca^{2+} in smooth muscle cells[8,35] and may promote the expression of pro-survival genes through activation of the transcription factor cyclic AMP response element binding[33].

NIHL is thought to be a result of the death of cochlear OHCs or damage to their mechano-sensory hair bundles[36,37]. However, it has been shown that moderate noise may also lead to the loss of afferent nerve terminals at the IHCs and a delayed degeneration of spiral ganglion neurons[2]. Synaptic ribbons couple to auditory nerve fibers at a ratio of 1:1 (ref. 38). We observed a reduction in ribbon numbers at the IHC synaptic pole in noise-exposed rats and mice, which is in line with previous reports[2]. Among the events that may cause loss of ribbons and afferent nerve terminals, harmful Ca^{2+} overload after noise exposure is a likely candidate. Indeed, activation of NO signaling in

IHCs was suggested to occur by Ca^{2+} influx through the ATP receptor $P2X_2$, which is activated by extracellular ATP after trauma[23,34]. Noise-induced activation of ATP receptors[25] and the subsequent activation of an extracellular signal-related kinase 1 (ERK1)-ERK2 cascade[30] has been suggested to cause harmful effects in mature IHCs. ERK1 and ERK2 can be modulated by cGMP and Prkg1 (ref. 39). Alternatively, or additionally, Prkg1 may prevent Ca^{2+} overload by the phosphorylation of the inositol triphosphate (IP_3)-receptor–associated Prkg1 substrate (IRAG) or of BKCa channels, which conduct the largest fraction of K^+ currents in mature IHCs[40].

We show that Pde5 and Prkg1 are expressed in neurons and that Prkg1 (if not both Prkg1 and Pde5) is expressed in the satellite cells of spiral ganglia. In both neuronal and non-neuronal cells, the protective effects of cGMP have been linked to its target, Prkg (for a review, see ref. 33).

The finding that vardenafil pretreatment increased PAR concentrations in Prkg1 control mice but not in Prkg1-deficient mice is particularly notable. Parp1 is a ubiquitously expressed DNA nick-end sensor that uses nicotinamide adenine dinucleotide (NAD^+) as a substrate to catalyze the addition of PAR to acceptor proteins, in particular histones, several transcription factors and Parp itself[41]. DNA breaks activate Parp, which facilitates transcription, replication and DNA base excision repair[42]. Paradoxically, the toxic effects of NO have been linked to DNA damage, excessive activation of Parp1[41,43] and subsequent cell death by NAD^+ depletion or ATP depletion[41,42]. In this context, Pde5 inhibition may augment the protective effects of cGMP signaling without promoting the potentially destructive effects of high concentrations of NO, in particular because Parp activation may also be caused directly by cGMP[20,44]. We show a pro-survival effect of vardenafil-induced elevation of PAR concentrations, which may mirror the anti-aging capacity of Parp[45]. Here, the vardenafil-induced elevation of PAR concentrations was accompanied by a healthy, 'rescued' phenotype, as shown by persistent Kcnq4 staining in the OHCs and the maintenance of ribbons in the IHC synapses. As ribbon counts are a metric for IHC afferent innervation[46] and ribbon loss presumptively occurs after noise-induced deafferentation[2], cGMP-Prkg1-Parp cascade activation in spiral ganglia and supporting cells may contribute to stabilization of the IHC synapse. The particular targets of the beneficial cGMP-Prkg1 cascade in IHCs, OHCs, SGNs and satellite cells are elusive. Nevertheless, the elevation of PAR concentrations in cochlear cells after vardenafil treatment and the lower concentration of PAR seen in Prkg1-deficient mice provide evidence for a pro-survival Parp activity downstream of cGMP-Prkg1 signaling in the cochlea, as has been predicted for neuronal cells[19]. Future studies may identify Parp acceptor proteins and investigate the participation of Parp in age-dependent hearing loss.

Recent publications suggested that Pde5 inhibitors may be involved in hearing loss in mice[47] and humans[48]. One study[48] describes a higher incidence of self-reported hearing impairment in the vardenafil user group (0.4%) as compared to the non-user group (0.3%). The evidence available to date regarding this issue is contradictory, because other studies[49,50] could not disclose a deleterious effect of sildenafil or vardenafil. Currently, there is no clinical study that examines the risks of acute, short-term application of Pde5 inhibitors in humans— a form of application as we are presenting it here. In this study, controlled 3-week treatment of rats with the Pde5 inhibitor vardenafil did not impair hearing (**Supplementary Fig. 7**). Nevertheless, care must be taken before applying these findings to humans. Additional studies in large numbers of Pde5-treated patients are needed to more

definitively understand the role of Pde5-inhibitors in hearing loss, particularly if the drugs are taken chronically.

In conclusion, this study shows the presence of a cGMP-Prkg1 signaling cascade in NIHL that prevents damage and degeneration in OHCs and IHC synapses. Furthermore, cGMP-Prkg1 signaling increases Parp activity, which presumably promotes DNA repair. Stimulation of this endogenous mechanism with the Pde5 inhibitor vardenafil prevents noise-induced hair-cell dysfunction and cell death. These findings are relevant for the development of therapies for NIHL, as Pde5 inhibitors are already in clinical use, suggesting easy translation into patients with NIHL. However, human application, in particular, prophylactic use for hearing disorders, cannot be recommended before an evaluation of the safety of the drug.

METHODS

Methods and any associated references are available in the online version of the paper at http://www.nature.com/naturemedicine/.

Note: Supplementary information is available on the Nature Medicine website.

AUTHOR CONTRIBUTIONS

M.J., F.P.-D., P.R., R.F., J.E., M.K. and L.R. designed the research. M.J., J.D., M.G., U.Z., S.W., K.V., H.X. and L.R. performed experiments. C.F. and M.K. conducted immunofluorescent microscopy and image analyses. H.-S.G. and K.R. provided technical support. A.G. and S.F. prepared mutant mice, designed primers and generated antibodies. J.E., N.B. and S.K. isolated hair cell tissues and contributed to the RT-PCR. P.R. and J.S. designed protein detection methods and provided antibodies for histology. J.H. and P.S. established drug application protocols in rats and provided the Pde5 inhibitor. M.K. and L.R. planned and supervised the project. M.J., F.P.-D., R.F., J.E., M.K. and L.R. wrote the manuscript, which was revised by all authors.

COMPETING FINANCIAL INTERESTS

The authors declare no competing financial interests.

Published online at http://www.nature.com/naturemedicine/ .

Reprints and permissions information is available online at http://www.nature.com/reprints/index.html .

1. Ruben, R.J. Development of the inner ear of the mouse: a radioautographic study of terminal mitoses. *Acta Otolaryngol. Suppl.* **220**, 221–244 (1967).
2. Kujawa, S.G. & Liberman, M.C. Adding insult to injury: cochlear nerve degeneration after "temporary" noise-induced hearing loss. *J. Neurosci.* **29**, 14077–14085 (2009).
3. Feil, R. & Kemp-Harper, B. cGMP signalling: from bench to bedside. Conference on cGMP generators, effectors and therapeutic implications. *EMBO Rep.* **7**, 149–153 (2006).
4. Conti, M. & Beavo, J. Biochemistry and physiology of cyclic nucleotide phosphodiesterases: essential components in cyclic nucleotide signaling. *Annu. Rev. Biochem.* **76**, 481–511 (2007).
5. Porst, H. *et al.* Efficacy and safety of tadalafil once daily in the treatment of men with lower urinary tract symptoms suggestive of benign prostatic hyperplasia: results of an international randomized, double-blind, placebo-controlled trial. *Eur. Urol.* **60**, 1105–1113 (2011).
6. Tian, F., Fessenden, J.D. & Schacht, J. Cyclic GMP-dependent protein kinase-I in the guinea pig cochlea. *Hear. Res.* **131**, 63–70 (1999).
7. Vaandrager, A.B., Hogema, B.M. & de Jonge, H.R. Molecular properties and biological functions of cGMP-dependent protein kinase II. *Front. Biosci.* **10**, 2150–2164 (2005).
8. Hofmann, F., Feil, R., Kleppisch, T. & Schlossmann, J. Function of cGMP-dependent protein kinases as revealed by gene deletion. *Physiol. Rev.* **86**, 1–23 (2006).
9. Thomas, M.K., Francis, S.H. & Corbin, J.D. Substrate- and kinase-directed regulation of phosphorylation of a cGMP-binding phosphodiesterase by cGMP. *J. Biol. Chem.* **265**, 14971–14978 (1990).
10. Valtcheva, N. *et al.* The commonly used cGMP-dependent protein kinase type I (cGKI) inhibitor Rp-8-Br-PET-cGMPS can activate cGKI *in vitro* and in intact cells. *J. Biol. Chem.* **284**, 556–562 (2009).
11. Johnson, S.L. *et al.* Position-dependent patterning of spontaneous action potentials in immature cochlear inner hair cells. *Nat. Neurosci.* **14**, 711–717 (2011).
12. van Wijk, E. *et al.* The *DFNB31* gene product whirlin connects to the Usher protein network in the cochlea and retina by direct association with USH2A and VLGR1. *Hum. Mol. Genet.* **15**, 751–765 (2006).
13. Hibino, H. *et al.* Expression of an inwardly rectifying K^+ channel, $K_{ir}4.1$, in satellite cells of rat cochlear ganglia. *Am. J. Physiol.* **277**, C638–C644 (1999).
14. Marcotti, W. & Kros, C.J. Developmental expression of the potassium current $I_{K,n}$ contributes to maturation of mouse outer hair cells. *J. Physiol. (Lond.)* **520**, 653–660 (1999).
15. Kharkovets, T. *et al.* Mice with altered KCNQ4 K^+ channels implicate sensory outer hair cells in human progressive deafness. *EMBO J.* **25**, 642–652 (2006).
16. Rüttiger, L. *et al.* Deletion of the Ca^{2+}-activated potassium (BK) α-subunit but not the BKβ1-subunit leads to progressive hearing loss. *Proc. Natl. Acad. Sci. USA* **101**, 12922–12927 (2004).
17. Engel, J. *et al.* Two classes of outer hair cells along the tonotopic axis of the cochlea. *Neuroscience* **143**, 837–849 (2006).
18. Chen, Y.S. *et al.* Changes of hair cell stereocilia and threshold shift after acoustic trauma in guinea pigs: comparison between inner and outer hair cells. *ORL J. Otorhinolaryngol. Relat. Spec.* **65**, 266–274 (2003).
19. Kim, Y.M. Nitric oxide protects PC12 cells from serum deprivation-induced apoptosis by cGMP-dependent inhibition of caspase signaling. *J. Neurosci.* **19**, 6740–6747 (1999).
20. Paquet-Durand, F. *et al.* Excessive activation of poly(ADP-ribose) polymerase contributes to inherited photoreceptor degeneration in the retinal degeneration 1 mouse. *J. Neurosci.* **27**, 10311–10319 (2007).
21. Lugnier, C. Cyclic nucleotide phosphodiesterase (PDE) superfamily: a new target for the development of specific therapeutic agents. *Pharmacol. Ther.* **109**, 366–398 (2006).
22. Uemaetomari, I. *et al.* L-type voltage-gated calcium channel is involved in the pathogenesis of acoustic injury in the cochlea. *Tohoku J. Exp. Med.* **218**, 41–47 (2009).
23. Shen, J., Harada, N., Nakazawa, H. & Yamashita, T. Involvement of the nitric oxide-cyclic GMP pathway and neuronal nitric oxide synthase in ATP-induced Ca^{2+} signalling in cochlear inner hair cells. *Eur. J. Neurosci.* **21**, 2912–2922 (2005).
24. Housley, G.D. *et al.* Expression of the $P2X_2$ receptor subunit of the ATP-gated ion channel in the cochlea: implications for sound transduction and auditory neurotransmission. *J. Neurosci.* **19**, 8377–8388 (1999).
25. Wang, J.C. *et al.* Noise induces up-regulation of $P2X_2$ receptor subunit of ATP-gated ion channels in the rat cochlea. *Neuroreport* **14**, 817–823 (2003).
26. Sugasawa, M., Erostegui, C., Blanchet, C. & Dulon, D. ATP activates non-selective cation channels and calcium release in inner hair cells of the guinea-pig cochlea. *J. Physiol. (Lond.)* **491**, 707–718 (1996).
27. Gale, J.E., Piazza, V., Ciubotaru, C.D. & Mammano, F. A mechanism for sensing noise damage in the inner ear. *Curr. Biol.* **14**, 526–529 (2004).
28. Shen, J. *et al.* Role of nitric oxide on ATP-induced Ca^{2+} signaling in outer hair cells of the guinea pig cochlea. *Brain Res.* **1081**, 101–112 (2006).
29. Murai, N. *et al.* Activation of JNK in the inner ear following impulse noise exposure. *J. Neurotrauma* **25**, 72–77 (2008).
30. Meltser, I., Tahera, Y. & Canlon, B. Glucocorticoid receptor and mitogen-activated protein kinases activity after restraint stress and acoustic trauma. *J. Neurotrauma* **26**, 1835–1845 (2009).
31. Takeda-Nakazawa, H. *et al.* Hyposmotic stimulation-induced nitric oxide production in outer hair cells of the guinea pig cochlea. *Hear. Res.* **227**, 59–70 (2007).
32. Wang, H., Kohr, M.J., Traynham, C.J. & Ziolo, M.T. Phosphodiesterase 5 restricts NOS3/soluble guanylate cyclase signaling to L-type Ca^{2+} current in cardiac myocytes. *J. Mol. Cell Cardiol.* **47**, 304–314 (2009).
33. Fiscus, R.R. Involvement of cyclic GMP and protein kinase G in the regulation of apoptosis and survival in neural cells. *Neurosignals* **11**, 175–190 (2002).
34. Shen, J., Harada, N. & Yamashita, T. Nitric oxide inhibits adenosine 5′-triphosphate-induced Ca^{2+} response in inner hair cells of the guinea pig cochlea. *Neurosci. Lett.* **337**, 135–138 (2003).
35. Pfeifer, A. *et al.* Defective smooth muscle regulation in cGMP kinase I-deficient mice. *EMBO J.* **17**, 3045–3051 (1998).
36. Liberman, M.C. & Dodds, L.W. Single-neuron labeling and chronic cochlear pathology. II. Stereocilia damage and alterations of spontaneous discharge rates. *Hear. Res.* **16**, 43–53 (1984).
37. Liberman, M.C. & Dodds, L.W. Single-neuron labeling and chronic cochlear pathology. III. Stereocilia damage and alterations of threshold tuning curves. *Hear. Res.* **16**, 55–74 (1984).
38. Fuchs, P.A. Time and intensity coding at the hair cell's ribbon synapse. *J. Physiol. (Lond.)* **566**, 7–12 (2005).
39. Komalavilas, P., Shah, P.K., Jo, H. & Lincoln, T.M. Activation of mitogen-activated protein kinase pathways by cyclic GMP and cyclic GMP-dependent protein kinase in contractile vascular smooth muscle cells. *J. Biol. Chem.* **274**, 34301–34309 (1999).

40. Kros, C.J., Ruppersberg, J.P. & Rusch, A. Expression of a potassium current in inner hair cells during development of hearing in mice. *Nature* **394**, 281–284 (1998).
41. Schreiber, V., Dantzer, F., Ame, J.C. & de Murcia, G. Poly(ADP-ribose): novel functions for an old molecule. *Nat. Rev. Mol. Cell Biol.* **7**, 517–528 (2006).
42. Yu, Z., Kuncewicz, T., Dubinsky, W.P. & Kone, B.C. Nitric oxide-dependent negative feedback of PARP-1 *trans*-activation of the inducible nitric-oxide synthase gene. *J. Biol. Chem.* **281**, 9101–9109 (2006).
43. Szabó, C. Poly(ADP-ribose) polymerase activation by reactive nitrogen species—relevance for the pathogenesis of inflammation. *Nitric Oxide* **14**, 169–179 (2006).
44. Sahaboglu, A. *et al. PARP1* gene knock-out increases resistance to retinal degeneration without affecting retinal function. *PLoS ONE* **5**, e15495 (2010).
45. Beneke, S. & Burkle, A. Poly(ADP-ribosyl)ation in mammalian ageing. *Nucleic Acids Res.* **35**, 7456–7465 (2007).
46. Liberman, M.C. Effects of chronic cochlear de-efferentation on auditory-nerve response. *Hear. Res.* **49**, 209–223 (1990).
47. Hong, B.N., Yi, T.H., Kim, S.Y. & Kang, T.H. High dosage sildenafil induces hearing impairment in mice. *Biol. Pharm. Bull.* **31**, 1981–1984 (2008).
48. McGwin, G. Jr. Phosphodiesterase type 5 inhibitor use and hearing impairment. *Arch. Otolaryngol. Head Neck Surg.* **136**, 488–492 (2010).
49. Giuliano, F., Jackson, G., Montorsi, F., Martin-Morales, A. & Raillard, P. Safety of sildenafil citrate: review of 67 double-blind placebo-controlled trials and the postmarketing safety database. *Int. J. Clin. Pract.* **64**, 240–255 (2010).
50. Maddox, P.T., Saunders, J. & Chandrasekhar, S.S. Sudden hearing loss from PDE-5 inhibitors: A possible cellular stress etiology. *Laryngoscope* **119**, 1586–1589 (2009).

ONLINE METHODS

Mice and rats. Care and use of the mice and rats and the experimental protocol were reviewed and approved by the animal welfare commissioner and the regional board for scientific animal experiments in Tübingen, Germany. We used female 3–5-month-old Wistar rats (Charles River) and 3–7-week-old female Prkg1-deficient mice carrying two *Prkg1* null alleles and littermate controls, which were generated as described previously[51].

Drug application. For the rat experiments, we dissolved vardenafil (Bayer) in ethanol, Solutol (BASF) and water at a ratio of 1:4:5 and administered this solution ten times in 12-h intervals by gavage (5 ml per kg of body weight).

For the mouse experiments, we administered vardenafil subcutaneously (10 mg per kg of body weight in a dilution of 10 mg and 10 ml water injection containing 15 μl ethanol) 1 h before noise exposure and then another nine times in 12-h intervals. For the rats and mice treated long term, vardenafil was administered orally. The vehicle solution did not contain vardenafil.

Hearing measurements. We performed the physiological recordings as described[17]. In short, we measured the ABRs to sound stimuli with 100-μs clicks and frequency-specific tone bursts of 3 ms duration. To record the ABRs, we inserted subdermal silver-wire electrodes at the vertex of and ventro-lateral to the measured ear. We defined thresholds as the sound pressure level where a stimulus-correlated response was identified by visual inspection of the averaged signal by an expert observer. We assessed OHC function by the growth function and the maximum response in the distortion product audiogram of the cubic DPOAE, as described[17]. Frequency pairs of tones were between f2 = 4 kHz and f2 = 32 kHz.

Noise exposure. We induced acoustic trauma by exposing anesthetized mice and rats to band noise free field in a reverberating chamber (rats, 4-16 kHz and mice, 4–16 kHz or 8–16 kHz, 120 dB SPL RMS for 1 h).

Tissue preparation. For RNA and protein isolation, cochleae were dissected, immediately frozen in nitrogen and stored at −80 °C before use[52]. For immunohistochemistry, we fixed, decalcified and sectioned the cochleae, as described[52]. For whole-mount preparation, we dissected cochlear turns and mounted them on slides with the tissue adhesive Cell-Tek (BD Bioscience) in PBS and performed immunohistochemistry as described[17].

Single OHC and IHC isolation. Apical and medial half turns of the organ of Corti from 5-week-old female control and Prkg1-deficient mice and from rats aged postnatal day 21–26 were dissected and fixed on a cover slip. We separately harvested OHCs and IHCs with micropipettes[53].

RT-PCR. We amplified Prkg1 with the oligonucleotides 5′-ACAACT GTACCCGGACAGCGA-3′ and 5′-TCCTCTTGCACCCTGCCTGAT-3′ by RT-PCR as described[54]. For single cells, we performed nested PCR with the oligonucleotides 5′-GAAACTCTGGGCCATCGATC-3′ and 5′-GGTCTC TTCGAGGAC-3′. For Prkg1 isoform-specific RT-PCR, we used the following oligonucleotides: Prkg1a, 5′-GAGGAAGAAATCCAGGAGC-3′ and 5′-TTT ACAACTGTACCCGGAC-3′, and for nested RT-PCR, 5′-CGCCAGGCG TTCCGGAAGT-3′ and 5′-AAGGCGTGAAGCTCTGCAC-3′; Prkg1b, 5′-AGGGAAAGTTGATCCGAGAGGGG-3′ and 5′-CGACATCCAGGAT CTCAGCCACG-3′, and for nested RT-PCR, 5′-GGGATTTACAGTATGCGCT CCAGGAG-3′ and 5′-ACGAACTGGACAAGTATCGCTCGGTG-3′. We amplified Pde5 in rats with the oligonucleotides 5′-AACGGCCCTGTGTACAATT CG-3′ and 5′-TGGTCGAAGTGATGGTGCTC-3′. The oligonucleotides used for nested PCR were 5′-GCCGATGGATTTTGAGTGTC-3′ and 5′-CCGCTGTA TGTATGAGTTGTT-3′. We did all PCR experiments in at least triplicate.

Immunohistochemistry. We performed immunohistochemistry as described[52] using primary specific antibodies to Kcnq4 (rabbit polyclonal, 1:50 (refs. 16,54)), Pde5 (rabbit polyclonal, 1:20, Cell Signaling Technology, 2395), Ctpb2 (mouse monoclonal, 1:50, BD Transduction Laboratories, 612044), neurofilament 200 (mouse monoclonal NF200, 1:8,000, Sigma, N5139), $K_{ir}4.1$ (mouse monoclonal, 1:100, Sigma, WH0003766M1), Eps8 (mouse monoclonal, 1:50, BD Transduction Labs, 61014), BKCa (rabbit, 1:50, Alomone Labs, APC-021) and whirlin (guinea pig polyclonal, 1:50 (ref. 12)). We detected the Prkg1 protein with a rabbit polyclonal antibody that recognizes both the Prkg1α and Prkg1β isoforms (general antibody to Prkg1) (1:50)[10] and the Prkg1β isoform with a selective rabbit polyclonal antibody[55] or a selective goat polyclonal antibody (1:50) (Santa Cruz Biotechnology, sc-10342). We repeated each labeling three times in at least three independent experiments. With the exception of Kcnq4 and BKCa staining, we derived all images of the fluorescent stainings from deconvoluted Z-stacks, as described[56]. We visualized hair cell stereocilia bundles by fluorescent phalloidin labeling of F-actin (570–573 nm, Sigma-Aldrich), as described[57]. We performed PAR immunostaining using antibodies specific to PAR (1:200) (Alexis, 804-220) as described[20,44].

Western blot. We performed western blot analysis as described[58] on cochlear tissue from 3-month-old rats and 5-week-old Prkg1-deficient mice. As additional controls, we loaded 2 ng of purified recombinant Prkg1α[59] and Prkg1β[60] protein. We incubated blotted proteins with rabbit polyclonal Prkg1 antiserum (1:2,000) that recognizes both Prkg1α and Prkg1β[10], antiserum that selectively recognizes the Prkg1α isoform (Santa Cruz Biotechnology, sc-10335) or the Prkg1β isoform (Santa Cruz Biotechnology, sc-10342) or rabbit polyclonal antibody specific to Pde5 (1:1,000) (Cell Signaling Technology, 2395).

Statistical analyses. Data were compared using Student's *t* test. For the dependent data of the time-course experiments, data were compared by MANOVA (JMP 9.00, SAS Institute). In the case of significance by MANOVA, we compared the data pairwise by Student's *t* test with α-level Bonferroni-Holm adjustment. Counts for Ctbp2 immunopositive ribbons and Parp-positive cells were compared by one-way ANOVA and by a *post hoc* Bonferroni's multiple comparison test (Prism 2.01, GraphPad Software). For the frequency-dependent ABR data, we used a *t* test and applied the Bonferroni-Holm α-level adjustment. For the OHC counting, we used a non-parametric Mann-Whitney U test. Normal distribution was tested by *F* test.

51. Wegener, J.W. *et al.* cGMP-dependent protein kinase I mediates the negative inotropic effect of cGMP in the murine myocardium. *Circ. Res.* **90**, 18–20 (2002).
52. Knipper, M. *et al.* Thyroid hormone deficiency before the onset of hearing causes irreversible damage to peripheral and central auditory systems. *J. Neurophysiol.* **83**, 3101–3112 (2000).
53. Michna, M. *et al.* Cav1.3 (α1D) Ca²⁺ currents in neonatal outer hair cells of mice. *J. Physiol. (Lond.)* **553**, 747–758 (2003).
54. Winter, H. *et al.* Thyroid hormone receptors TR-α1 and TR-β differentially regulate gene expression of Kcnq4 and prestin during final differentiation of outer hair cells. *J. Cell Sci.* **119**, 2975–2984 (2006).
55. Geiselhöringer, A., Gaisa, M., Hofmann, F. & Schlossmann, J. Distribution of IRAG and cGKI-isoforms in murine tissues. *FEBS Lett.* **575**, 19–22 (2004).
56. Zampini, V. *et al.* Elementary properties of Caᵥ1.3 Ca²⁺) channels expressed in mouse cochlear inner hair cells. *J. Physiol. (Lond.)* **588**, 187–199 (2010).
57. Hahn, H., Müller, M. & Löwenheim, H. Whole organ culture of the postnatal sensory inner ear in simulated microgravity. *J. Neurosci. Methods* **171**, 60–71 (2008).
58. Schug, N. *et al.* Differential expression of otoferlin in brain, vestibular system, immature and mature cochlea of the rat. *Eur. J. Neurosci.* **24**, 3372–3380 (2006).
59. Feil, R., Kellermann, J. & Hofmann, F. Functional cGMP-dependent protein kinase is phosphorylated in its catalytic domain at threonine-516. *Biochemistry* **34**, 13152–13158 (1995).
60. Ruth, P. *et al.* Identification of the amino acid sequences responsible for high affinity activation of cGMP kinase Iα. *J. Biol. Chem.* **272**, 10522–10528 (1997).